

# Effects of the MHz Frequency Range Electromagnetic Immunity of the Swept Frequency Pulse Coupled on the kHz Frequency Range G3 Power Line Communication

1<sup>st</sup> Aarsh Nateghi  
Electromagnetic Effects and HPEM  
Bundeswehr Research Institute for  
Protective Technologies and NBC  
Protection (WIS)  
Munster, Germany  
nateghi@geml.uni-hannover.de

2<sup>nd</sup> Niek Moonen  
Power Electronics and EMC  
(EEMCS)  
University of Twente  
Enschede, The Netherlands  
niek.moonen@utwente.nl

3<sup>rd</sup> Martin Schaarschmidt, 4<sup>th</sup> Sven Fisahn  
Electromagnetic Effects and HPEM,  
Bundeswehr Research Institute for  
Protective Technologies and NBC  
Protection (WIS), Munster, Germany  
{MartinSchaarschmidt,  
SvenFisahn}@bundeswehr.org

5<sup>th</sup> Heyno Garbe  
Institute of Electrical Engineering and  
Measurement Technology  
Leibniz Universität Hannover  
Hannover, Germany  
garbe@geml.uni-hannover.de

**Abstract**—This contribution evaluates the vulnerability of narrowband power line communication in the kHz frequency range through the implementation of frequency swept pulse intentional electromagnetic interference (IEMI) in the MHz frequency range. For this experiment, different types of digital modulation as well as different types of transmission mode are evaluated. The data frame error rate of the transmitter and receiver are compared when a low power frequency-swept pulse IEMI is coupled to the G3 power line communication. Finally, a mitigation plan to manage the risk of intentional EMI in power line communications is recommended.

**Keywords**— IEMI, Power Line Communication, PLC, EMI, Smart-Grid Communication, G3 PLC, Frequency-Swept Pulse

## I. INTRODUCTION

The G3 power line communication (G3-PLC) has as many uses in smart cities, for instance in smart metering, building automation, electric mobility, railways and smart grid control and monitoring. Smart devices require an intelligent method of communication and the G3-PLC offers the ability to send and receive data in a wide variety of applications. According to the European Committee for Electro-technical Standardisation CENELEC, the frequency bandwidth of the G3-PLC is set to range from 3 kHz to 148 kHz [1].

In [2] the effect of LED lamps on narrow-band G3-PLC for the CENELEC-A frequency band of 9-95 kHz was assessed and, with 32 lamps installed in the same circuit, a frame error rate FER of 13, 3% observed.

The method of spread spectrum modulation (SSM) to reduce the effects of the converter circuit in PRIME-PLC CENELEC-A narrowband communication was also evaluated in [3]. The results show that spread spectrum actually can have a more devastating effect than actually mitigating the issue.

These types of PLC test boards, which can work with both PRIME and G3-PLC, are standardised and offer tailor-made solutions for different applications. The environmental electromagnetic emissions from LED lamps [2] or converter switching pulses [4] can be recognised, examined and attenuated or filtered. The two papers mentioned earlier deal with the unintended EMI effects, while the novelty of this

experiment lies in the intended EMI version, which can intelligently disturb the PLC channel with less power.

Furthermore, the focus of this article is to evaluate the effect of the Frequency Swept Pulse (FSP) signal with spectral content in a much higher frequency range, MHz range, coupled into the G3-PLC channel with a communication frequency range of 35 kHz to 90 kHz.

The following paragraphs in Section II provide two methods for defining the FSP signal as the source of IEMI. The associated measurement setup, including the measurement technology, is explained in Sections III.A and III.B. A method of coupling the generated IEMI to the G3-PLC channel is then assessed in Section III.C. Considering different types of transmission parameters such as modulation type and transmission mode, Section IV analyses the effects of the FSP-IEMI signal on the data frame transmission rate of the G3-PLC PHY layer. Next, Section V outlines a systematic mitigation plan to minimize the IEMI effects. Finally, Section VI summarises the overall message of this article.

## II. RELATED WORK

This section describes methods for generating FSP signals with Matlab, which can be fed to a programmable arbitrary wave generator (PAWG) and also to a less intelligent AWG. After comparing both methods, critical elements of the IEMI signal in the MHz frequency range, which cause the interferences in the kHz frequency range of the PLC, can be more clearly uncovered.

### A. FSP Signal as defined by Matlab

Sweeping through a pulse signal changes the frequency of the pulse signal generated depending on the type of sweep function. For this work, a linear sweep over a pulse with a 50% duty cycle is used. The mathematical model of the FSP signal is given in Equations (1) and (2).

$$u(t) = V \frac{\tau}{T} + \frac{2V}{\pi} \sum_{n=1}^{\infty} \left( \frac{1}{n} \sin \left( \pi n \frac{\tau}{T} \right) \cos(2\pi n f t) \right) \quad (1)$$

where,  $f = \frac{1}{T}$ ,  $\tau$ (pulse width) = 50 %,  $V = 19 \text{ V}$ ,  $0 < t < SP$



<sup>1</sup>The research leading to these results has received funding from the European Union's Horizon 2020 research and innovation programme under the Marie Skłodowska-Curie grant agreement No 812.790 (MSCA-ETN PETER). This publication reflects only the authors' view, exempting the European Union from any liability. Project website: <http://etn-peter.eu/>.

$$f_0(t) = \frac{d}{dt} [f(t)t] = \frac{f_2 - f_1}{SP} t + f_1, \quad (2)$$

where;  $f_1 = 8.014$  MHz,  $f_2 = 8.081$  MHz and Sweep Period(SP) = 2 ms, Sampling frequency ( $f_s$ ) = 1.014 MHz

The Sweep Period (SP) is defined according to the subcarrier spacing, which is an important part of the Orthogonal Frequency Division Multiplex (OFDM) communication of multi-carrier modulation (MCM) [5]. The jamming signal used for PLC test boards is similar to the jamming signal used in [6].

The FSP signal and associated power spectrum are plotted by Matlab and shown in Figure 1.

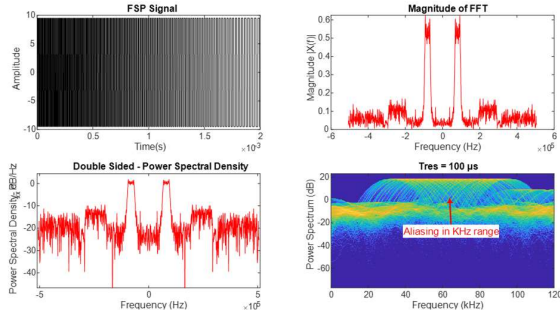


Figure 1. IEMI FSP signal from Equations (1) and (2).

As can be seen from Figure 1, the FSP signal with a sampling frequency ( $f_s$ ) of 1.014 MHz, which is less than the Nyquist frequency point, causes the signal to be aliased. The signals that have fallen apart can then be shifted to other frequency bands and cause unforeseen intentional interference in the PLC channel if they are defined by the programmable AWG and intentionally coupled into the transmission line.

### B. FS Pulse generated by an arbitrary waveform generator

In addition to the FS pulse generated by Matlab and PAWG, the non-programmable AWG is used to generate an FSP signal whose start and stop frequencies ( $f_1$  and  $f_2$ ) match Equation (2). A pulse signal is swept over a period of two milliseconds in the MHz frequency range, the sampling frequency being automatically selected by AWG. To get the right effect from the MHz frequency of the pulse signal over the kHz spectrum, the exact selection of  $f_1$  and  $f_2$  is required, as shown in Figure 2 below, compared to a signal defined by Matlab showing the selection of the correct sampling frequency could lead to a similar result.

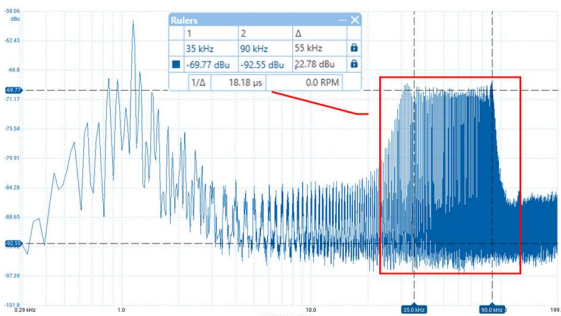


Figure 2. FSP signal generated by AWG on the transmitter side.

The amplitude of the spectral power density of FSP signals in Figure 1 and Figure 2 (power spectrum/frequency,

bottom right diagram) is approximately equal around 20 dBu. However, the amplitude will drop due to transmission losses when the FSP IEMI signal is injected into the PLC channel.

## III. TEST SETUP

This section describes the test tools to demonstrate the FSP IEMI signals defined in the previous section and the test equipment to monitor and analyse G3-PLC network performance. The general structure of the test and measurement setup for performing the wired IEMI on the G3- PLC channel is shown in Figure 3.

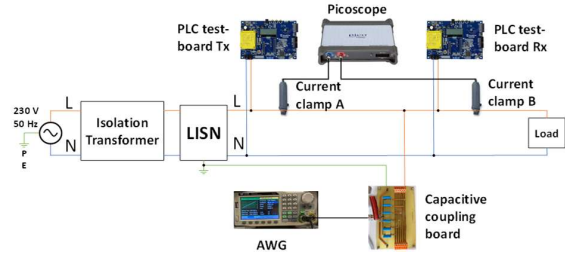


Figure 3. Measurement setup layout.

From Figure 3, the isolating transformer and the Line Impedance Stabilisation Network (LISN) are connected in series in order to protect the local network from conducted FSP IEMI signal and to filter the noises from local network into the test setup.

### A. G3-PLC connection

Two ATPL360-EK PLC-standardised Microchip test boards, Transmitter (Tx) and Receiver (Rx), are connected to the network to be tested after the LISN connection in order to provide an end-to-end communication link.

### B. Measurement setup

A Picoscope 5000 series is used to measure the current flowing through the line conductor (L) using N2783B current clamps, one near the Tx and the other one near the Rx side of the network.

### C. Source of IEMI and coupling circuit

The FS pulse signal explained in Section II.B is generated by the T3FG120 AWG and coupled to the G3-PLC network via a capacitive coupling board (Figure 4).

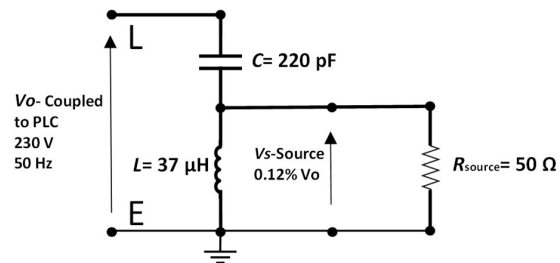


Figure 4. Capacitive coupling board.

### D. Frame Error Rate (FER)

The impact of IEMI on the G3-PLC circuit is monitored and analysed by the Microchip PLC PHY Tester Tool and the ratio of the corrupted data frame to the total data sent from Tx to Rx is calculated from Equation (3) [2].

$$FER = \left( \frac{\text{Data frame corrupted}}{\text{Total data frame sent}} \right) \cdot 100 \% \quad (3)$$

All digital modulation types available on the test board (BPSK, QPSK, 8PSK, ROB\_BPSK) as well as various transmission modes are evaluated. For all options, the total number of frames selected is 1000 and the time interval is 100 ms.

In addition, the transmission modes are varied: very low impedance, very high impedance and automatic selection by the device when an inductive coupling auxiliary device with 311  $\mu\text{H}$ , 15 A is added to the transmission line. The inductor used emulates the distance between transmitter and receiver of G3-PLC modems to approximately 200 meters as shown in Figure 5 below.

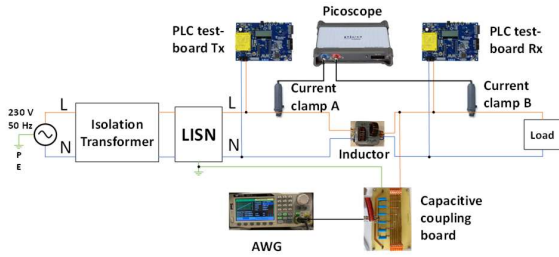


Figure 5. Measurement setup layout including added inductor.

The results of the measurement and the associated analysis are listed in Section IV below.

#### IV. MEASUREMENT RESULTS

Figure 6 below shows how the FS-Pulse-IEMI signal corrupts the G3-PLC channel by covering the data transfer bandwidth for one of the combined options mentioned in previous Section III; QPSK modulation and 200 meters distance between PLC modems.

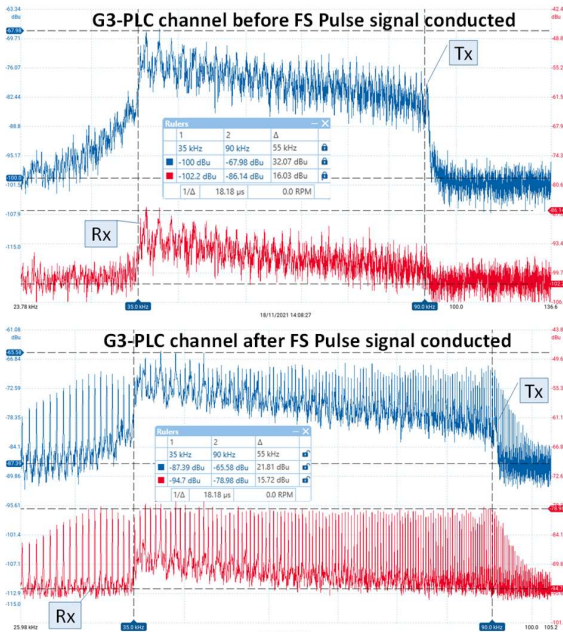


Figure 6. G3-PLC signal before and after FSP IEMI signal coupled.

From Figure 7, due to the large distance of 200 meters between Tx and Rx, the average power of the Rx signal is

approximately 16 dBu less than that of the Tx signal. As a result of the conducted FS Pulse IEMI signal nearby Tx side of the transmission, the power spectrum of the Tx is covered more than the Rx signal along the signal bandwidth of 35 kHz to 90 kHz of the G3-PLC channel (Tx: 32 – 21 = 11 dBu and Rx: 16 – 15 = 1 dB).

The comparison of the data frame error rate for different types of modulation and transmission modes for the duration of the FS Pulse IEMI signal, which is coupled into the G3- PLC communication channel, is shown in Table I.

TABLE I. FER FROM G3-PLC VARIOUS TYPES OF MODULATION AND TRANSMISSION MODES FOR THE COUPLED IEM FSP SIGNAL.

| Modulation Type | Transmission Mode                   | Tx_Frame_Error % | Rx_Frame_Error % |
|-----------------|-------------------------------------|------------------|------------------|
| BPSK            | Very Low Impedance                  | 30.54            | 35.50            |
| QPSK            | Very Low Impedance                  | 32.27            | 33.51            |
| 8PSK            | Very Low Impedance                  | 30.20            | 33.51            |
| ROB_BPSK        | Very Low Impedance                  | 30.20            | 33.51            |
| BPSK            | High Impedance                      | 47.71            | 48.36            |
| QPSK            | High Impedance                      | 46.84            | 47.27            |
| 8PSK            | High Impedance                      | 46.41            | 47.05            |
| ROB_BPSK        | High Impedance                      | 34.77            | 40.05            |
| BPSK            | Auto selection (200 meter distance) | 45.13            | 45.13            |
| QPSK            | Auto selection (200 meter distance) | 55.03            | 55.03            |
| 8PSK            | Auto selection (200 meter distance) | 50.82            | 50.82            |
| ROB_BPSK        | Auto selection (200 meter distance) | 45.13            | 45.13            |

As can be seen from Table I, the QPSK-type PLC modulation has the highest FER when the impedance for the 200 meter distances between Tx and Rx is very high. The very low impedance transmission mode of the PLC test boards has the lowest FER and the ROB\_BPSK modulation type is more robust than other modulation types when the EMI signal is routed to the PLC channel. The frame transmission behaviour for two of given scenarios from Table I (ROB BPSK very low impedance and QPSK 200 meter distance) are shown in Figure 7 below.

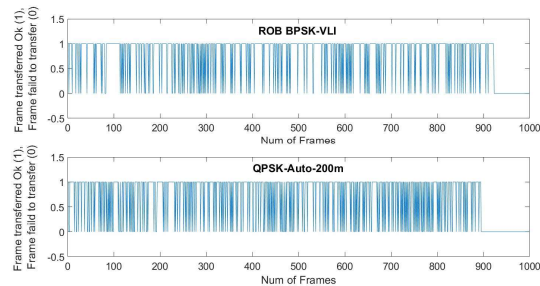


Figure 7. FER behaviour for two scenarios.

As can be seen from Figure 7, the correctly received data frames drop to zero after 900 frames in the case of a QPSK 200 meter distance scenario, indicating a complete loss of data transmission. Overall, the consequence of 30 to 50%



data loss for critical infrastructures such as smart grid communication systems can have a major impact on system operation. Therefore, a comprehensive mitigation plan needs to be established to minimise the risk of IEMI disturbing the G3-PLC channel.

## V. MITIGATION PLAN RECOMMENDED

The standardised methods of IEMI risk management include the use of standard test kits and the demonstration of methods provided by standard regulators. With the rapid increase in the complexity of electronic and communication technologies, it may not be possible to consider only the rule-based methods associated with reducing the risk of electromagnetic interference.

In [7] the systematic approach of TSECA (a threat scenario of the effects and criticality analysis) to the analysis and management of the risk of IEMI is explained. Due to the simplification and explanation of the individual steps of risk management with this method and also the consideration of the standards as the basis of the risk assessment, a combination of a rule-based and a risk-based approach is recommended. A summary of the steps of the TSECA process is shown in Figure 8 below.

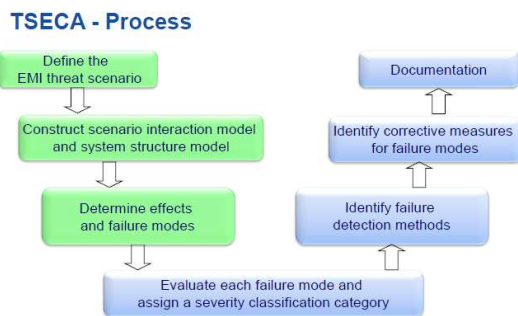


Figure 8. TSECA process blk diagram [7].

The first three steps of the TSECA process from Figure 8 are implemented in this work and described in the previous sections.

In addition, due to the complexity of the data analysis, which includes technical and non-technical inputs [8], a statistical data analysis approach such as the probabilistic risk analysis technique (e.g. Monte Carlo simulation technique) can support the IEMI risk analysis [9].

## VI. CONCLUSION AND NEXT WORK

From this article, the effects of FS Pulse EMI in the MHz range, which is coupled into the G3-PLC-PHY layer in the kHz frequency range, is assessed. In addition, the sampling frequency and the exact magnitude of  $f_1$  and  $f_2$  of the sweep period have a direct effect on the shift in the frequency bandwidth of the FS Pulse signal over the G3-PLC channel in order to disturb the data transmission frame rate. The data frame error rate of G3-PLC channel can vary due to the change in modulation type and transmission mode during an IEMI attack. The IEMI can be coupled to both Tx and Rx sides of the PLC. If there is a large distance between two PLC modems, the disruptive effect on Rx side can be lower in compare with Tx side due to the positioning of IEMI injection on Tx side. The modulation type of QPSK has the highest data

frame error rate over long distance compared to the other types tested for this experiment. The vulnerability of the G3-PLC channel is proven with just a simple method, using an AWG and a capacitive coupling board, where the EMI signal has not even been amplified. In order to reduce the impact of the IEMI risk, technical inputs such as electrical breakdown failure should be included in the probabilistic assessment (such as the Monte Carlo simulation). In addition, assessing the IEMI risk of a complex smart grid communication system requires the probability of different outcomes from different scenarios when random variables, such as the modulation types or distance between Tx and Rx, intervene. Additionally, the impact of risks and uncertainties in the forecasting model needs to be assessed as part of the mitigation plan, which required a multi-dimensional Monte-Carlo simulation design to include both technical and non-technical elements of the IEMI risk. The next step after this experiment is the planned access to a complex smart grid communication network, which is considered a critical infrastructure. Then the susceptibility of the entire system to radiated and conducted IEMI signals, especially the Wi-Fi and PLC communication channels, can be tested. Finally, a systematic and probabilistic risk-based IEMI assessment can be carried out.

## VII. REFERENCES

- [1] K. Razazian, M. Umari, A. Kamalizad, V. Loginov and M. Navid, „G3-PLC specification for powerline communication: Overview, system simulation and field trial results“, *ISPLC2010, 2010*, pp. 313-318, doi: 10.1109/ISPLC.2010.5479881.
- [2] M. A. Wibisono, N. Moonen and F. Lefterink, „Interference of LED Lamps on Narrowband Power Line Communication“, *2020 IEEE International Symposium on Electromagnetic Compatibility & Signal/Power Integrity (EMCSI)*, 2020, pp. 219-221, doi: 10.1109/EMCSI38923.
- [3] W. El Sayed, P. Crovetto, N. Moonen, P. Lezynski, R. Smolenski and F. Lefterink, „Electromagnetic Interference of Spread-Spectrum Modulated Power Converters in G3-PLC Power Line Communication Systems“, *in IEEE Letters on Electromagnetic Compatibility Practice and Applications*, vol. 3, no. 4, pp. 118-122, Dec 2021, doi: 10.1109/LEMCPA.2021.3121091.
- [4] W. El Sayed, P. Crovetto, P. Lezynski, R. Smolenski, A. Madi and F. Grassi, „The Influence of Commercial PC Switched Mode Power Supply Interference on the PRIME PLC Performance“, *2021 IEEE International Joint EMC/SI/PI and EMC Europe Symposium, 2021*, pp. 632-636, 2021, doi: 10.1109/EMC/SI/PI/EMCEurope52599.2021.9559175.
- [5] al, C. Shahriar et, „PHY-Layer Resiliency in OFDM Communications: A Tutorial“, *IEEE Communications Surveys & Tutorials, Firstquarter 2015*, vol. 17, no. 1, pp. 292-314, doi: 10.1109/COMST.2014.2349883.
- [6] A. Nateghi, M. Schaarschmidt, S. Fisahn and H. Garbe, „Vulnerability of Wireless Smart Meter to Electromagnetic Interference Sweep Frequency Jamming Signals“, *2021 IEEE International Joint EMC/SI/PI and EMC Europe Symposium, 2021*, pp. 755-759, 2021, doi: 10.1109/EMC/SI/PI/EMCEurope52599.2021.9559200.
- [7] Sabath, F, „A systematic approach for electromagnetic interference risk management“, *in IEEE Electromagnetic Compatibility Magazine, Fourth Quarter 2017*, vol. 6, no. 4, pp. 99-106, doi: 10.1109/EMEC.0.8272296.
- [8] M. Lanzrath, M. Suhrke and H. Hirsch, „HPEM-Based Risk Assessment of Substations Enabled for the Smart Grid“, *in IEEE Transactions on Electromagnetic Compatibility*, vol. 62, no. 1, pp. 173-185, Feb. 2020, doi: 10.1109/TEMC.2019.2893937.
- [9] E. Genender, H. Garbe and F. Sabath, „Probabilistic Risk Analysis Technique of Intentional Electromagnetic Interference at System Level“, *in IEEE Transactions on Electromagnetic Compatibility*, vol. 56, no. 1, pp. 200-207, Feb 2014, doi: 10.1109/TEMC.2013.2272944.